



SEISMIC RESPONSE OF HIGH-STRENGTH STEEL REINFORCED CONCRETE FRAMES

L. Laughery⁽¹⁾, S. Pujol⁽²⁾

⁽¹⁾ Graduate Research Assistant, Purdue University, llaugher@purdue.edu

⁽²⁾ Professor, Purdue University, spujol@purdue.edu

Abstract

Substituting conventional reinforcing steel bars with high-strength steel bars can reduce reinforcement congestion, improve constructability, and lower costs in reinforced concrete construction. Member dimensions remaining the same, high-strength steel reinforced concrete (HSSRC) members have lower post-cracking stiffness compared to conventionally-reinforced members of comparable strength. The subject of this investigation is whether this reduction in post-cracking stiffness results in higher peak drifts in structures containing HSSRC members. Four portal frames with identical member dimensions, but different column longitudinal reinforcement configurations, were tested on a unidirectional earthquake simulator. Two frames (type C) had conventional steel longitudinal reinforcement in the columns. In the other two frames (type H), a reduced ratio of high-strength steel was used as column longitudinal reinforcement to achieve comparable nominal strength. Reinforcing details of the frames were otherwise the same. Each frame was subjected to a series of five ground motions of either increasing or decreasing intensity. Measurements of their response showed that peak drifts of type H frames were comparable to drifts of type C frames. It was also observed that softening caused by damage from previous shaking did not affect peak drift, suggesting that initial period of vibration dominated frame response.

Keywords: reinforced concrete; high-strength steel; shake table; simulated earthquakes

1. Introduction

American Concrete Institute (ACI) standards are used around the world for the design of reinforced concrete structures. ACI's "Building Code Requirements for Structural Concrete" (ACI 318) currently limits the yield strength of longitudinal reinforcement to 60 ksi or less [410 MPa or less] for structures expected to resist seismic demands [1]. This requirement can lead to constructability problems in reinforced concrete (RC) members where large amounts of steel are needed to resist prescribed demands. Substituting high-strength steel for conventional longitudinal steel can mitigate these problems while maintaining member strength (for members with equal dimensions). Before this substitution can be implemented, members containing high-strength steel longitudinal reinforcement must be studied.

The design of structures encompasses two sides: capacity and demand. The capacity of high-strength steel reinforced concrete (HSSRC) members has long been a subject of investigation. Dozens of quasi-static tests to measure the deformation capacity of HSSRC members have been conducted since the early 1960s ([2][3][4][5], among others). By comparison, the drift demand on HSSRC members during earthquakes has received little attention.

All other factors remaining the same, if high-strength steel is substituted (in reduced amounts) for conventional steel in a RC member, the result is a member with: (a) comparable initial stiffness and (b) comparable nominal strength, but (c) lower post-cracking stiffness. Past numerical investigations of RC buildings subjected to strong ground motions indicate that the lower post-cracking stiffness in HSSRC frames (compared to conventional RC frames) does not lead to consistently higher roof drift [5]. The tests conducted in this investigation seek to evaluate this experimentally. That is, they seek to evaluate whether lower post-cracking stiffness will have an impact on the peak drift response of HSSRC frames subjected to strong ground motions.

2. Experiments

The objective of the experiments described here was to compare the peak drift response of two reinforced concrete systems with comparable initial stiffness and nominal strength, but different post-cracking stiffnesses. To achieve this, four reinforced concrete portal frames were built. The frames had the same member dimensions, but two different column longitudinal reinforcement configurations. Two frames of each type were built. Each frame was tested five times on a unidirectional earthquake simulator. This simulator was used at the University of Illinois Urbana-Champaign from the 1970s through the 1990s to study the response of RC structures to simulated earthquakes [6].

2.1 Specimens

An elevation view of a typical specimen is shown in Fig. 1. The specimens were portal frames with an out-of-plane thickness of 5 in. [130 mm]. The columns were square with a height of $h = 42$ in. [1067 mm]. The top and bottom beams were 10 in. [254 mm] and 12 in. [305 mm] deep. In contrast to the typical strong-column weak-beam technique used in seismic design, the frames were designed with columns that were weaker than the beams. This was meant to force the response of the system to be driven by the columns.

Member dimensions were the same in all four frames, and identical reinforcement configurations were used in the top and bottom beams. Only column longitudinal reinforcement differed (Fig. 1). In columns in type C frames, four 3/8-in. [9.5 mm] deformed steel reinforcing bars were used as longitudinal reinforcement. This provided a longitudinal reinforcement ratio, ρ_l , of 1.8%. Here, ρ_l is defined as:

$$\rho_l = (A_s + A_s')/A_g \quad (1)$$

where A_s is area of steel in tension, A_s' is area of steel in compression, and A_g is gross cross-sectional area. This steel had a yield stress of 65 ksi [450 MPa] and a strength of 100 ksi [690 MPa]. In columns in type H frames, four 1/4-in. [6.5 mm] high-strength undeformed steel reinforcing bars were used as longitudinal reinforcement ($\rho_l = 0.8\%$). This steel had a yield stress of approximately 160 ksi [1100 MPa] and a strength of nearly 190 ksi [1300 MPa]. Neither steel had a well-defined yield plateau, so the yield stresses reported above are based on the

0.2% offset method. To improve bond with the concrete, the high-strength bars were corroded before casting. This was done by cleaning the bars to remove oil, spraying a 10% solution of hydrochloric acid (HCl) on their surfaces, and then storing the bars for 72 hours in a moist room.

Reinforcement details are illustrated in Fig. 2. Longitudinal reinforcement was anchored in the beams using hooks with an embedment length of 22 in. [560 mm]. In type H frames, these hooks also terminated in assemblies comprised of plates and cast-in anchor chucks. This was done to prevent slip of the reinforcing steel in the beams, which was a concern due to the lack of surface deformations and high anticipated bond stresses for the small bars. Shear reinforcement was provided in the columns at a spacing of $d/4$ to a distance of $3d$ from the face of beams ($d = \text{effective depth} = 4 \text{ in. [102 mm]}$), and approximately $d/2$ elsewhere along the column height.

All frames were cast on the same day and using the same mortar mix. The mix had a maximum aggregate size of $3/8 \text{ in. [9.5 mm]}$. Detailed proportions of the mix are specified in Table 1. The average compressive strength across all test days was 3800 psi [26.2 MPa]. The modulus of elasticity of the concrete (E_c) was measured as the secant modulus to 40% of the stress at ultimate load. This definition was selected not because it was considered better than alternative definitions, but because it is commonly used in industry. Using this definition, the average modulus of elasticity for all tests was $E_c = 2700 \text{ ksi [18.6 MPa]}$.

2.2 Setup

Each frame was tested by itself on a unidirectional earthquake simulator. The test setup is illustrated in Fig. 3. The setup was instrumented with 4 accelerometers, 10 displacement transducers, and 64 NDI Optotrak[®] optical markers. These markers captured the motion of the simulator, setup components, and frame in three dimensions. In addition, 2 DSLR cameras captured video of the tests from different angles. Data from the tests are available at datacenterhub.org/resources/14094. This dataset includes measurements from the sensors, as well as photos, videos, and crack maps of the specimens.

Prior to testing, a reusable concrete mass was connected to the top beam of each frame. This mass, the top beam, and hardware used to connect them had a combined weight of approximately 4800 lb [2200 kg]. Including the weight from the upper two-thirds of the columns [7], the effective mass of the system was calculated to be 5000 lb [2270 kg]. It was assumed that the columns would resist lateral demand in flexure, with an initial stiffness of $k_i = 2 \cdot 12E_c I_g / h^3$ where I_g is the gross moment of inertia of a single column. Based on this assumption and the mentioned effective mass, the calculated initial period of the frames was $T_i = 0.1 \text{ sec}$.

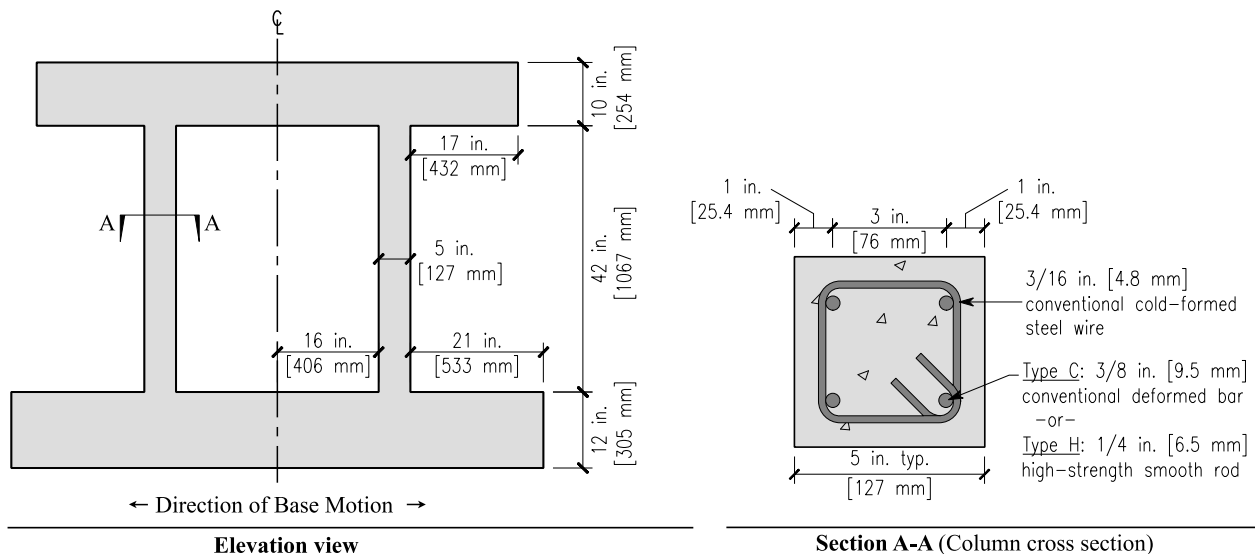


Fig. 1 – Elevation view of test specimen and cross sections of columns.

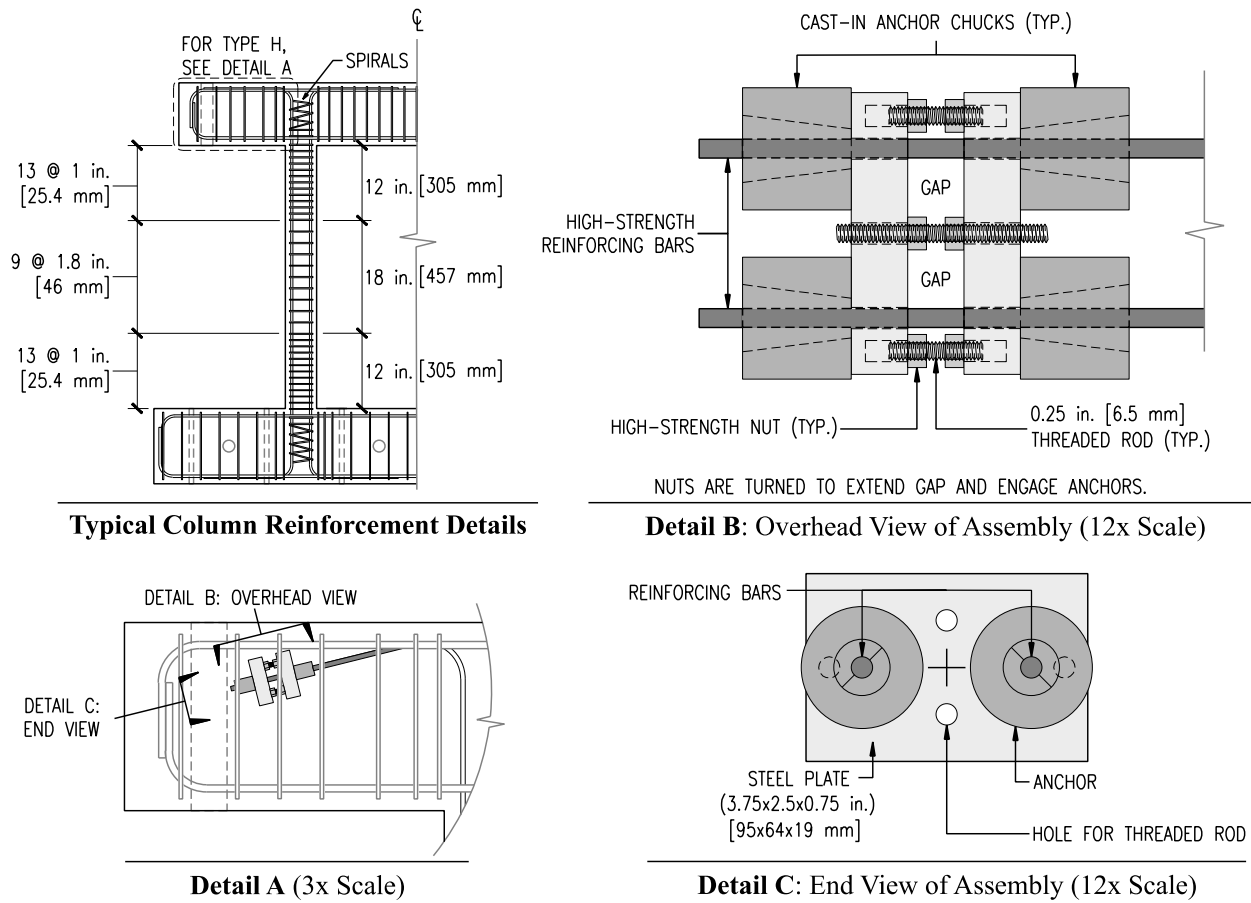


Fig. 2 – Longitudinal reinforcement details and anchorage assemblies used in type H frames.

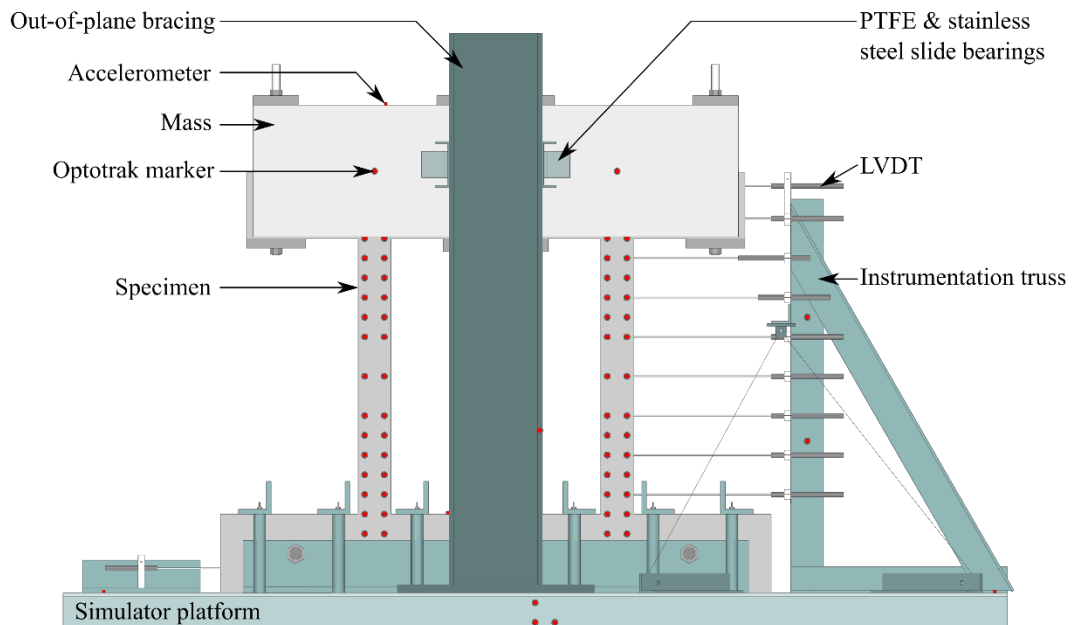


Fig. 3 – Test setup.

Table 1 – Mix proportions of grout used in specimens per cubic yard (CY) [1 CY = 0.765 m³].

Material	#23 Sand	Cement	Water
Weight, lb [kg]	2760 [1250]	620 [280]	410 [185]
Specification [Ref. Nr.]	ASTM C33 [8] & INDOT 2014 Standard Specification §904.02h [9]	ASTM C150, Type I [10]	–

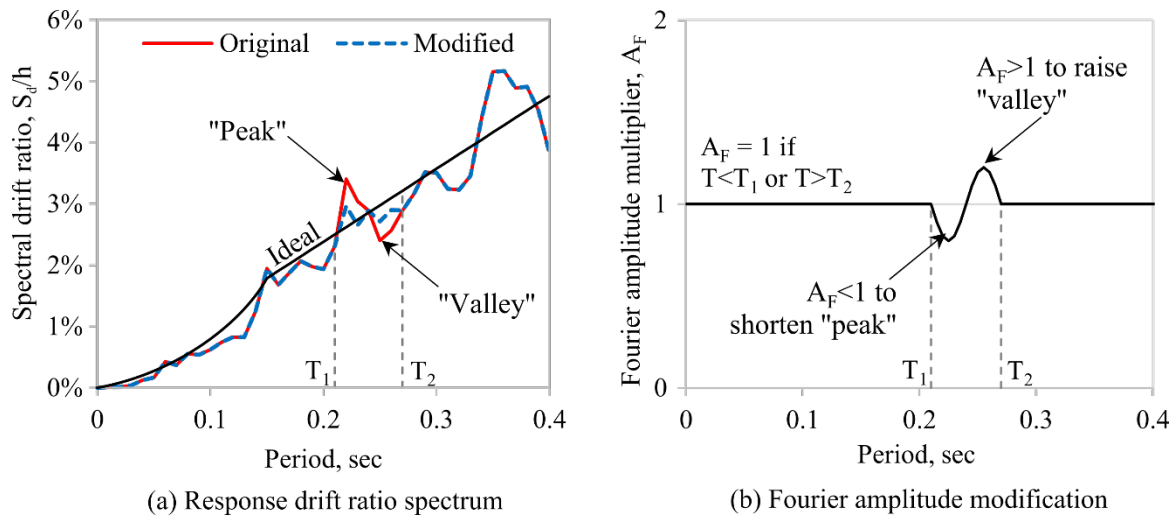


Fig. 4 – Illustration of Fourier spectrum modification process.

2.3 Test Program

Each frame was subjected to five simulated ground motions. These motions were scaled versions of the east-west component of the record obtained at Roscoe Boulevard Station during the 1994 Northridge earthquake. This record was compressed in time by dividing the original time step (0.01 sec) by a factor of 3. Accelerations were multiplied by factors as large as 3.9. The resulting acceleration record was modified so that its displacement response spectrum matched the idealized spectrum [Fig. 4(a)] more closely. This was done by reducing the prominence of “peaks” and “valleys” in the spectrum. To do so, acceleration records were transformed into the Fourier domain, and the amplitudes were adjusted at periods where “peaks” and “valleys” were observed. For example, if a peak was observed at $T = 0.22$ sec, then the Fourier amplitude corresponding to that peak was reduced by multiplying by a factor $A_F < 1$ [Fig. 4(b)]. For valleys the Fourier amplitude was multiplied by a factor $A_F > 1$. The result was an acceleration history that produced a displacement response spectrum closer to the idealized displacement response spectrum.

The strongest of the resulting motions (which we refer to as the 100% motion) had a peak ground acceleration (PGA) of 1 g, a peak ground velocity (PGV) of 11 in./sec [280 mm/sec], and a peak ground displacement (PGD) of 1.3 in. [33 mm]. Motions of smaller intensity were obtained by reducing the amplitude of this “100%” motion by multiplying its accelerations by 0.75 (75%), 0.5 (50%), and 0.25 (25%). The response spectra for all motions used are shown in Fig. 5.

Two test series were conducted. In series 1, frames C1 and H1 were subjected to four ground motions of increasing intensity (25%, 50%, 75%, 100%), followed by a repeat of the 100% motion. In series 2, frames C2 and H2 were subjected to ground motions of decreasing intensity (100%, 75%, 50%, and 25%), followed by a repeat of the 100% motion. This was done to examine the effect of damage and softening from prior ground motions on peak drift response. In past investigations, RC frames which experienced ground motions (and damage as a result) have been observed to reach comparable peak roof drifts to identical (but undamaged) frames subjected to the same ground motion, provided that this motion was the strongest the frames had

experienced [11][12]. This suggests that damage and softening may not have an impact on peak drift response of RC frames.

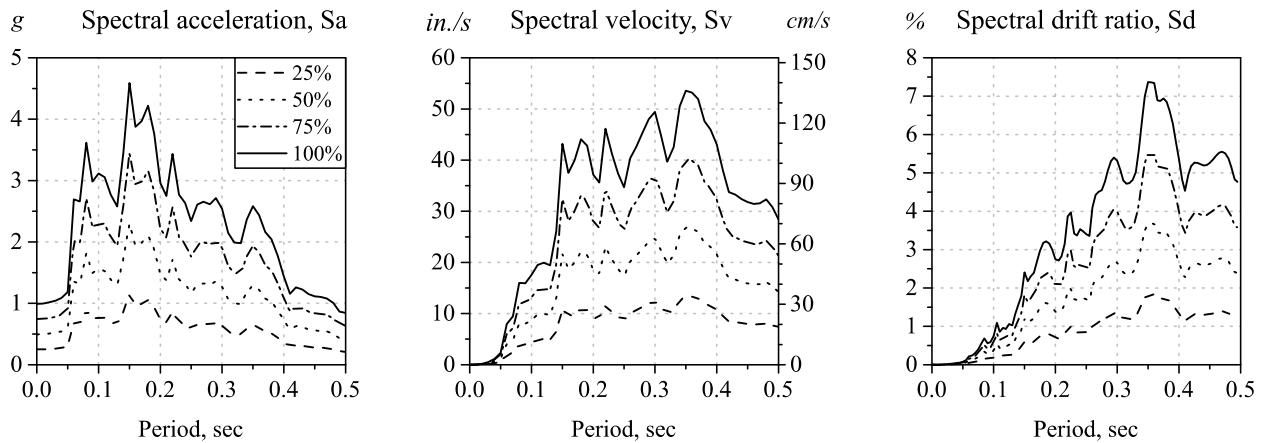


Fig. 5 – Linear response spectra for ground motions used in this investigation (2% critical damping).

3. Results & Discussion

The initial period of the frames was determined by measuring the response of the frames to: (1) impact hammer tests, and (2) platform jolt when the simulator was first turned on. Based on these measurements, the initial period of the frames was approximately 0.12 sec for type H and 0.15 sec for type C.

A summary of recorded PGAs and PGVs derived from table acceleration histories during the tests is presented in Table 2. These values indicate that the ground motions to which the specimens were subjected were consistent at each intensity.

3.1 Force-displacement Envelopes

Force-displacement envelopes were generated starting from the equation of motion at points of zero velocity:

$$m(\ddot{x} + \ddot{z}) + kx = 0 \Big|_{\dot{x}=0} \tag{2}$$

where m is mass, x is relative lateral displacement at the top, z is base displacement, and k is stiffness. Dots above terms denote derivatives with respect to time. Using Eq. (2), force-displacement plots were constructed for each test. The y-axis [lateral inertial force, first term in Eq. (2)] was obtained as the product of the effective mass and absolute acceleration measured at the top of the specimens. The x-axis (drift) was obtained from the displacement transducers at the top of the frame. This term includes permanent deformation from prior motions (e.g. it is cumulative drift, as opposed to in-run drift). For each frame, the uppermost points of these plots were connected to create a force-displacement envelope (Fig. 6). These envelopes show that type H frames had lower post-cracking stiffness than type C frames. They also show that type H frames developed less lateral resistance than type C frames at their peak displacement, even though the two frames were expected to have approximately the same strength.

Table 2 – Summary of peak ground acceleration (PGA) and peak ground velocity (PGV) for each test.

Intensity	PGA, g				PGV, in./sec [mm/sec]			
	Series 1		Series 2		Series 1		Series 2	
	C1	H1	C2	H2	C1	H1	C2	H2
25%	0.86	0.86	0.89	0.93	3.7 [94]	3.4 [86]	3.5 [89]	3.4 [86]
50%	1.5	1.3	1.3	1.4	6.9 [175]	6.5 [165]	6.9 [175]	6.3 [160]
75%	1.6	1.8	1.9	1.7	9.0 [229]	9.1 [231]	9.2 [234]	9.0 [229]
100% (1)	2.1	2.0	2.6	1.9	11.3 [287]	11.6 [295]	11.9 [302]	11.4 [290]

100% (2)	2.0	2.0	2.0	1.9	11.8 [300]	11.4 [290]	11.8 [300]	11.1 [282]
----------	-----	-----	-----	-----	------------	------------	------------	------------

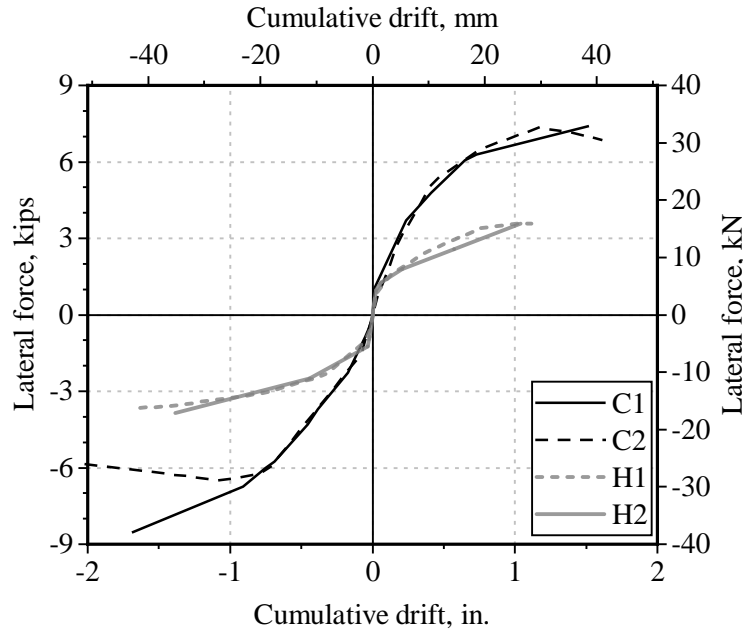


Fig. 6 – Lateral force-drift envelopes.

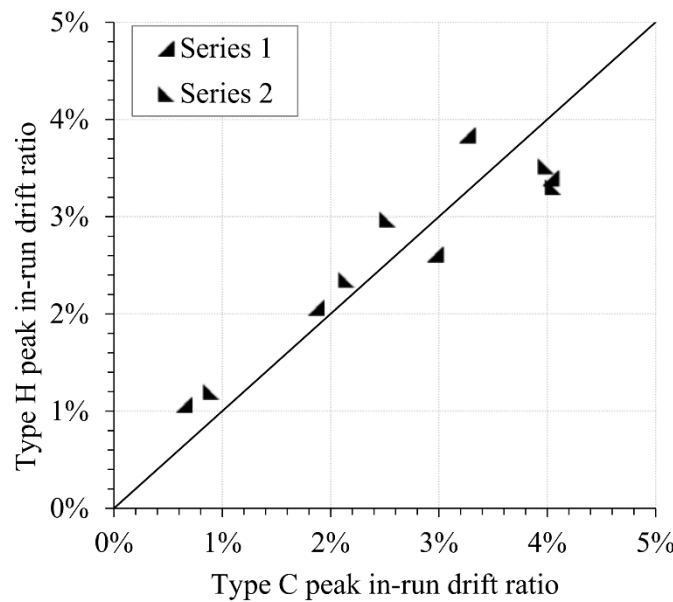


Fig. 7 – Comparison of peak in-run drift ratios for type C and type H frames.

The lower lateral resistance reached by type H frames can be related to debonding of the high-strength longitudinal reinforcement along the height of the columns. The longitudinal bars in the columns needed to develop their strength from the expected point of inflection at column mid-height to the beam-column joint (a length of 21 in. [533 mm]). Assuming uniform bond along this length, this would require the high-strength bars to develop bond stresses of more than 500 psi [3.5 MPa] at yield and nearly 600 psi [4.1 MPa] at ultimate. In the past, maximum bond stresses on the order of 450 psi [3.1 MPa] have been observed for plain bars, with slip starting at 60% of this value [13].

Slip of the high-strength bars along the height of the column would have distributed elongation in the steel over the entire column height, reducing steel strain and consequently, stress. This would have resulted in lower lateral stiffness. Observed crack patterns of the frames support the idea that slip occurred. In type C frames, cracks were observed along the full height of the columns, indicating that the reinforcing steel engaged the surrounding concrete. In contrast, in type H frames cracks were observed only at the tops and bottoms of the columns. Had the high-strength steel bonded with the surrounding concrete, tensile strain would have led to cracking along the length of the columns in type H frames, as it did in type C frames.

As a result of slip, the post-cracking stiffness of type H frames was lower than anticipated on the basis of the moment of inertia of cracked cross sections. This reduction in stiffness made the experiments more demanding tests of the idea that post-cracking stiffness does not control peak drift response. Although slip reduced the lateral resistance of type H frames in the range of drifts reached in the tests, mechanical anchors in the beams ensured that the nominal strength was attainable at larger drifts than those reached.

3.2 Peak Drift Response

A comparison of peak drifts for type C and H frames is presented in Fig. 7. Drift ratios ranged from 0.6% during the weakest ground motion to 4% during the strongest. For the weakest motion (25% intensity), the coefficient of variation across all frames was 26%. For other intensities, the coefficient of variation was on the order of 10%. This suggests that the lower post-cracking stiffness and lateral resistance of type H frames was not detrimental to their drift response.

The order of testing also had little effect on peak drift. For example, consider the first 100% motion. Prior to this test, series 1 frames (C1 and H1) had been subjected to 3 ground motions of lower intensity and experienced drift ratios up to approximately 3%. Series 2 frames (C2 and H2) were “pristine,” having experienced no previous ground motion. When subjected to the first 100% ground motion, frames C1 and C2 both reached peak drifts of approximately 1.7 in. [43 mm]. Similarly, frames H1 and H2 both reached peak drifts of approximately 1.4 in. [36 mm] during this ground motion.

4. Conclusions

The objective of this investigation was to test whether two reinforced concrete frames with comparable initial stiffness and nominal strength, but different post-cracking stiffnesses, would reach comparable peak drift during a given ground motion. Two types of frame were tested on an earthquake simulator. One contained conventional longitudinal reinforcement in the columns (type C), and the other contained a reduced amount of high-strength longitudinal reinforcement (type H). The two types of frame were designed to have the same nominal strength, but during the tests type H frames reached lower resistance than type C frames in the range of drifts reached. Although type H frames had lower post-cracking stiffness than type C frames, and although they developed smaller resisting forces, they reached comparable peak drifts during the same ground motions. Damage and softening from prior ground motions also had no appreciable impact on the peak drift response of the frames for stronger motions. Those frames which had experienced more ground motions previously (or ground motions of larger intensity) did not consistently reach higher drifts than those which had not, supporting the idea that frames with similar initial stiffness reach similar drifts during a given ground motion.

5. Acknowledgements

This research would not have been possible without the support of our sponsors. Thanks are due to Cascade Steel and MMFX for donating the high-strength steel rod, Precision-Hayes International for donating cast-in anchor chucks, and Voss Engineering, Inc. for donating slide bearings for the test setup.

6. References

- [1] ACI Committee 318 (2014): *Building Code Requirements for Structural Concrete*. American Concrete Institute, Farmington Hills, MI, 524 pp.
- [2] Hognestad, E (1961): High strength bars as concrete reinforcement, Part 1 – Introduction to a series of experimental reports. *Journal of the PCA Research and Development Laboratories*, **3** (3), 23-29.
- [3] Yotakhong, P (2003): *Flexural Performance of MMFX Reinforcing Rebars in Concrete Structures*. MS Thesis, North Carolina State University. 145 pp.
- [4] Tavallali, H (2011): *Cyclic Response of Concrete Beams Reinforced with Ultrahigh Strength Steel*. PhD Thesis, The Pennsylvania State University. 311 pp.
- [5] Rautenberg, J (2011): *Drift Capacity of Concrete Columns Reinforced with High-Strength Steel*. PhD Thesis, Purdue University. 263 pp.
- [6] Sozen, M, Otani, S, Gulkan, P, Nielsen, N (1969): The University of Illinois Earthquake Simulator. *Proceedings, Fourth World Conference on Earthquake Engineering, Santiago, Chile*, **3**, 139-150.
- [7] Biggs, J (1964): *Introduction to Structural Dynamics*. Mc-Graw Hill. 341 pp.
- [8] ASTM C33 (2013): *Standard Specification for Concrete Aggregates*. American Society for Testing and Materials, West Conshohocken, PA. 11 pp.
- [9] INDOT (2014): *Standard Specifications*. Indiana Department of Transportation, Indianapolis, IN. 1074 pp.
- [10] ASTM C150 (2012): *Standard Specification for Portland Cement*. American Society for Testing and Materials, West Conshohocken, PA. 9 pp.
- [11] Otani, S, Sozen, M (1972): Behavior of Multistory Reinforced Concrete Frames During Earthquakes. *Civil Engineering Studies, Structural Research Series*, University of Illinois, **392**. 551 pp.
- [12] Cecen, H (1979): *Response of Ten Story, Reinforced Concrete Model Frames to Simulated Earthquakes*. PhD Thesis, University of Illinois at Urbana-Champaign. 337 pp.
- [13] Abrams, D (1913): Tests of Bond Between Concrete and Steel. *University of Illinois, Engineering Experiment Station Bulletin 71*. **11** (15). 240 pp.